



Published in final edited form as:

Biopolymers. 2016 August ; 105(8): 449–462. doi:10.1002/bip.22836.

Activation of G proteins by GTP and the mechanism of G α -catalyzed GTP hydrolysis

Stephen R. Sprang

Center for Biomolecular Structure and Dynamics, Division of Biological Sciences, University of Montana, 32 Campus Drive, Missoula, MT 59812, Telephone: (406) 243-6028, Fax: (406) 243-6024, stephen.sprang@umontana.edu

Introduction

Heterotrimeric G protein alpha subunits (G α), recognized first as regulatory GTPases activated by β adrenergic receptors and rhodopsin, were discovered over forty years ago^{1–6}. Within ten years the archetypal members of the family – G α_s , G α_i and transducin (G α_t) had been purified and enzymatically characterized^{7–12}. More than twenty years ago, the first three-dimensional structures of G α subunits were described in GTP, GDP and heterotrimeric states^{13–20}. Yet, only recently, with the advent of the crystal structure of the β_2 -adrenergic receptor:Gs complex²¹ have we begun to clearly understand how G protein-coupled receptors release GDP from the nucleotide binding site from G α , leading to its activation.

Among guanine nucleotide binding proteins of the Ras superfamily, heterotrimeric G protein alpha subunits (G α) constitute a distinct group²². G α are unique with respect to their tertiary and quaternary structure, mechanisms of activation and signal transduction and in their kinetic properties. Like all members of the Ras superfamily, G α subunits are composed of a six-stranded parallel β core in which most successive strands are connected by α helices (Figure 1). The guanine nucleotide binding sites of these proteins are similar in structure and, to a lesser extent, in amino acid sequence to those of other members of the Ras superfamily^{22, 23}. Thus, the nucleotide binding sites of G α proteins are characterized by a guanine recognition motif, a P-loop that envelops the α and β phosphates of GTP and two dynamic structural elements called switch I and switch II that respond to the presence or absence of the GTP γ phosphate (Figure 2, Table 1). Two residues, a serine in the P-loop and a threonine in switch II coordinate Mg²⁺, which bridges the β and γ phosphates of GTP. In contrast to small G proteins of the Ras family, Mg²⁺ binds with nanomolar affinity to GTP-bound forms of G α - it is present in all such complexes described in this review - but only weakly, with affinity in the millimolar range, to the GDP state^{10, 24}. Both switch elements contain catalytic residues that participate in the mechanism of GTP hydrolysis. The switches themselves undergo conformational changes upon conversion of GTP to GDP. Unique to G α subunits is the insertion, within switch I, of a ~120 residue α -helical domain, and the presence of additional switch regions (III and IV) that participate in effector/regulator binding or show state-dependent conformations²⁵. The helical domain plays a

regulatory role in the retention of guanine nucleotide, and contributes to $G\alpha$ class-specific recognition of effectors and regulators. Roles of the helical domain in the regulatory and catalytic functions of $G\alpha$ subunits continue to be discovered²⁶.

$G\alpha$ regulatory activity is tightly integrated with that of heterodimers formed by G protein beta and gamma subunits ($G\beta\gamma$). The canonical, non-signaling state for both $G\alpha$ and $G\beta\gamma$ exists in the form of a heterotrimer composed of GDP-bound $G\alpha$ and $G\beta\gamma$. As for Ras GTPases, $G\alpha$ is “activated” for interaction with effectors when bound to GTP, and deactivated by its intrinsic GTPase activity – which, for most $G\alpha$ proteins, is accelerated by GTPase activating proteins or protein domains (GAPs). Heterotrimeric G proteins are directly activated by integral membrane proteins (G protein-Coupled Receptors: GPCRs) that are stimulated by extracellular agonists^{27, 28}. Cells that express heterotrimeric G proteins thereby monitor external stimuli to direct their metabolic, secretory and transcriptional programs, regulate electrical conductivity and control cellular motility. To a first approximation, the effector specificity and amino acid sequence identity of $G\alpha$ subunits segregates the family into four distinct classes: *s* (activation of adenylyl cyclases), *i* (inhibition of certain adenylyl cyclase isoforms), *q/11* (phospholipase β activation) and *12/13* (activation and plasma membrane localization of Rho guanine nucleotide exchange factors (GEFs)). The catalog of effectors listed above exemplifies $G\alpha$ class specificity but is by no means exhaustive. $G\beta\gamma$ heterodimers have their own regulatory targets (e.g., G protein-regulated inward rectifying potassium channels) and in some instances are co-regulators of $G\alpha$ effectors (e.g., certain isoforms of adenylyl cyclase isoforms and phospholipase β)^{29–31}. Most $G\alpha$ subunits are reversibly localized at the membrane by palmitoylation at residues near their N-termini, and members of the $G\alpha_i$ subfamily are also N-terminally myristoylated^{32, 33}. Myristoylation increases $G\alpha_i1$ affinity for adenylyl cyclase, $G\beta\gamma$ subunits³⁴ and the cytosolic GEF/chaperone Ric-8A³⁵, rather than necessarily promoting membrane interaction. Hydrogen-deuterium exchange experiments indicate myristoylation alters secondary structure dynamics of $G\alpha_i1$ ³⁶.

In this review I am generally concerned with activated, GTP bound $G\alpha$ subunits: how the energy of GTP binding is utilized, and how its hydrolysis alters the regulatory capacity of $G\alpha$. In particular, I focus on the mechanism of $G\alpha$ -catalyzed GTP hydrolysis, and the means by which the slow intrinsic GTPase activity of $G\alpha$ is accelerated by GAPs. The forgoing introduction provides only a minimal foundation for our discussion of the role GTP binding and the mechanism of its hydrolysis. While no single review encompasses the complexity of G protein signaling, several provide starting points for more in-depth explorations^{22, 25, 37–41}.

$G\alpha$ •GTP in effector activation

The energy of GTP binding is used to prevent $G\alpha$ from interacting with $G\beta\gamma$ in a way that would prevent either species from expressing its regulatory functions. However, GTP does not in all cases cause full dissociation of $G\alpha$ from $G\beta\gamma$ ^{42, 43}. GTP also stabilizes $G\alpha$ for optimal interaction with effectors. Crystal structures reveal a variety of $G\alpha$ -effector binding interfaces^{44–47, 48, 49}. Central to all, however, is a binding scaffold composed of switch II, an irregular helix, and $\alpha 3$ (Figure 3). Parallel to each other and separated by 12–14Å, the two

helices form a spacious groove into which structural elements of the effector penetrate. The stability of this binding surface depends on the conformation of switch II, an inherently dynamic structure, which is disordered in the crystal structures of GDP-bound states of G α i¹⁷ and G α 12⁵⁰. Yet even in the GDP-bound complex of G α , switch II can support a productive interaction with effectors. A catalytic domain construct of adenylyl cyclase is weakly activated by G α s•GDP⁵¹, and PDZRhoGEF forms a stable complex with G α 13•GDP, albeit with lower affinity than with G α 13 bound to the slowly hydrolyzing GTP analog, guanosine-5'-O-3-thiophosphate (GTP γ S)⁵². However, in the GTP-bound state, Switch II becomes more rigid, as is evident from several crystal structures^{15, 16, 53}. Even in the GTP-bound state, switch II is a dynamic structure: electron spin resonance studies of G α i1 harboring a spin-label near the middle of switch II show that it exhibits fast anisotropic motion in solution⁵⁴. Nevertheless, electrostatic and hydrogen bonding interactions between the γ phosphate of GTP and amide groups at its N-terminus tip the balance from global disorder to dynamic order in Switch II. These hydrogen bonds presumably pay the entropic cost of packing interactions between switch II and side-chains of the underlying β -sheet scaffold, which in turn affords stronger interactions with effectors.

The mechanism of G α -catalyzed GTP hydrolysis

The kinetic properties of most G α subunits were well established nearly thirty years ago^{5, 22, 39}. Single turnover rates at 30 °C are in the range of 2–4 min⁻¹ for most classes of G α ⁵, but lower for G α q (0.8 min⁻¹)⁵⁵ and G α z (0.1 min⁻¹)⁵⁶. Yet, these sluggish GTPases are still remarkably efficient, with k_{cat}/K_M for some exceeding 10⁵, and comparable to the catalytic efficiencies of “average” enzymes⁵⁷. This surprising result is the consequence of the micromolar affinity of G α for its substrate GTP, which is reduced to nanomolar affinity in the presence of the Mg²⁺ co-factor¹⁰, far lower than the physiological concentration of either component⁵⁸. However, many of the physiological responses – particularly those related to ion channel regulation - require rapid signal termination that far exceeds the intrinsic rate of G α GTPase activity⁵⁹. That this catalytic activity can be further stimulated by effectors (PLC- β on G α q) and “regulators of G protein signaling” (RGS) domains, indicates that the catalytic potential of the G α GTPase site is not fully realized within the architecture of the protein itself.

The catalytic sites of Ras superfamily proteins, including G α , are well conserved²³ (Table 1) and hence the basic elements of the catalytic mechanism are likely to be the same for both families²⁵. Two amino acids were identified as essential to G α GTPase activity²² (Figure 2). Near the amino terminus of switch II, a glutamine residue (at position 204 in G α i1 and 227 in G α s) hereafter referred to as Gln_{cat}, is essential for catalytic activity. The conserved arginine residue in switch I (Arg 201 in G α s, Arg 178 in G α i1), hereafter Arg_{cat}, is also a major determinant of catalytic activity. The catalytic roles of Gln_{cat} and Arg_{cat} were not fully appreciated until structures of the complexes of G α i1 and Gat with GDP, Mg²⁺ and AlF₄⁻ were determined.

Fluoride ion had long been known to stimulate adenylyl cyclase activity⁶⁰, and possibly associated with GTP-dependent regulatory activity^{4, 61}, but it was not until experiments were conducted with purified proteins that G α , in the presence of Mg²⁺, was confirmed as the

target of fluoride activation⁶². A critical, but cryptic companion of these ions was discovered by neutron activation analysis to be Al^{3+} - a contaminant in disposable borosilicate glass test tubes and in preparations of ATP used in adenylyl cyclase assays⁶³. Together, these ions increase the intrinsic tryptophan fluorescence of GDP-bound $\text{G}\alpha$, a property characteristic of the GTP-activated state⁶⁴. The prescient hypothesis that the activating species is aluminum tetrafluoride, which functions as an analog of a γ phosphate moiety in $\text{G}\alpha\cdot\text{GDP}$ ⁶⁵, was shown to be consistent with ^{19}F NMR titration experiments. These indicated a stoichiometry of $\text{Mg}^{2+}\text{AlF}_n$ where $n=3$ or 4 , the latter giving rise to the AlF_4^- anion and the former, the neutral trifluoride⁶⁶. Further studies of the pH and $[\text{F}^-]$ dependence of activation suggested $\text{AlF}_3(\text{OH}^-)$ to be the more likely species⁶⁷. For brevity, I shall henceforth refer to all relevant AlF_n species as AIF. The second row element Be, as BeF_3^- or $\text{BeF}_2(\text{OH})^-$, also activates $\text{G}\alpha\cdot\text{GDP}$ in the presence of Mg^{2+} ^{63, 67}. Similarly, at millimolar concentrations, Mg^{2+} and F^- are capable of inducing the activated state of $\text{G}\alpha\cdot\text{GDP}$ in the absence of Al^{3+} ⁶⁸. Two Mg^{2+} ions and three to four F^- are required for activation. Although the structure of this complex has not been experimentally verified, it is likely that, one Mg^{2+} , like Be^{2+} , forms a trifluoride ion - mimicking a γ phosphate - while the second reprises its role in $\text{G}\alpha\cdot\text{GTP}$ complexes by bridging the β phosphate and a fluoride ligand of MgF_3^- . In all instances, metal (Al^{3+} , Be^{2+} , or Mg^{2+}) fluoride complexes mimic the γ phosphate monoanion.

The crystal structures of $\text{GDP}\cdot\text{Mg}^{2+}\cdot\text{AlF}_4^-$ (hereafter, $\text{GDP}\cdot\text{MgAIF}$)-bound $\text{G}\alpha$ and $\text{G}\alpha$ are illuminating. AIF appears to be a mimic, not of a γ -phosphate, but rather of a penta-coordinate transition state or intermediate for phosphoryl transfer^{14, 69}. In these complexes, the aluminate has four equatorial fluoride (or possibly three fluoride and one hydroxyl) ligands and two axial oxygen ligands, one being the β phosphorus and the other a water molecule, referred to as W_{nuc} . This water molecule occupies the position expected for the nucleophile engaged in an in-line attack on the γ phosphate. All of the aluminate ligands, including the axial species, are located 1.9–2.1 Å from the metal center. Particularly informative is the reorientation of Arg_{cat} and Gln_{cat} (Figure 2c) allowing the carboximido moiety of the latter to form hydrogen bonds with a fluoride substituent of AIF that mimics a γ phosphate oxygen atom, and with W_{nuc} . Arg_{cat} forms electrostatic interactions with the pro-S β phosphate oxygen and one of the fluoride substituents of AIF. Although $\text{GDP}\cdot\text{MgAIF}$ provides a model of the transition state, it does not elucidate the catalytic mechanism for GTP hydrolysis.

It is important to point out that the majority of experimental, and all of the computational studies of G protein-catalyzed GTP hydrolysis have focused on Ras, or the Ras:Ras-GAP complex. The latter is particularly relevant in the present context, in that it conserves all of the catalytic features found in the catalytic sites of $\text{G}\alpha$ subunits. Dubbed the “arginine finger”, Arg_{cat} is provided by Ras-GAP, where it is positioned to interact with the β - γ bridging oxygen of the GDP leaving group⁷⁰. The hypothesis, based on modeling and domain complementation experiments, that Arg_{cat} in the catalytic site of $\text{G}\alpha$ is a functional analog of the Ras-GAP “arginine finger” turns out to be exactly correct⁷¹. The Ras:Ras-GAP complex has been crystallized with $\text{GDP}\cdot\text{MgAIF}$ (as the trifluoroaluminate) at the active site of Ras, in which form the complex is most stable⁷². The catalytic site of the latter is quite similar to that of $\text{G}\alpha$ bound to $\text{GDP}\cdot\text{MgAIF}$ (as the tetrafluoroaluminate).

At least three events must take place in the course of G α -catalyzed GTP hydrolysis: 1, the catalytic site must undergo a preorganization step to support the transition state for phosphoryl transfer; 2, depending on the reaction mechanism, an intermediate or transition state for phosphoryl transfer develops; 3, a proton is transferred from the attacking water nucleophile to the γ phosphate leaving group. These steps can, in principle, be stepwise or concerted. A minimal catalytic scheme can be written as:



where G \cdot GTP represents the G α Michaelis complex with GTP and Mg²⁺. For G α , catalytic site preorganization (transition to G* in the reaction scheme) encounters an activation energy barrier on the order of 3–4 Kcal/mol, as deduced from the rate enhancement provided by G α GAPs of the Regulator of G protein Signaling (RGS) domain family and discussed in more detail below. In ground state structures of G α crystallized with GTP γ S or guanosine-5'-($\beta\gamma$ -imido)triphosphate (GppNHp) (Figure 2a,b), both Gln_{cat} and Arg_{cat} exhibit elevated thermal parameters, indicating that they undergo constrained dynamic motion. The average positions of these residues are not always the same in the GTP γ S complexes of different G α proteins^{15, 53, 69}. In particular, the 1.5Å crystal structure of G α i1 \cdot GppNHp is unusual in that both Gln_{cat} and Arg_{cat} are highly constrained in conformations that would appear to impede their respective roles in catalysis (Figure 2b)⁷³. In all of these structures, an ordered water molecule is located about 3.8Å from the γ phosphorus and distal to the β - γ bridging oxygen. Occupying a position consistent with its potential role as W_{nuc}, this ordered water forms a hydrogen bond with a γ -phosphate oxygen, but is offset from the axis of in-line attack (Figure 2a). The structure of the pre-organized state for G α \cdot GTP is not known, but likely shares features with crystal structures of G α \cdot GDP \cdot MgAlF, described in a preceding paragraph (Figure 2c). Warshel and coworkers have proposed that the catalytic role of Gln_{cat} in Ras is largely allosteric, aiding in the preorganization of the enzyme-substrate complex^{74, 75}. Indeed, the AlF-bound G α structures clearly show that Gln_{cat}, together with the main chain carbonyl oxygen of Thr 181 (G α i1 numbering, and equivalent to Ras Thr 35) positions W_{nuc} for in-line attack, thus providing up to two orders of rate acceleration, even for a loose transition state⁷⁶. As discussed below, an important role of G α GAPs is to maneuver Gln_{cat} into a catalytically functional orientation, as exemplified by the GDP \cdot MgAlF complexes. More global allosteric effects of Gln_{cat} upon the conformation of the enzyme active site itself appear to be subtle. Root mean square differences in the positions of main-chain P-loop atoms in the 1.5Å-resolution structure of G α i1 \cdot GppNHp relative to the corresponding 2.2Å-resolution structure of the GDP \cdot MgAlF complex are less than 0.15Å. However, in the GDP \cdot MgAlF complex of G α i1, switch II shifts slightly away from the nucleotide, such that the amide nitrogen of Gly 203 is displaced by 0.2Å from the γ phosphorus relative to its position in G α i1 \cdot GppNHp. This slight enlargement of the γ phosphate subsite appears to be a consequence of the rotation of the Gln_{cat} to its catalytically functional conformation in the AlF complex, and may preorganize the enzyme for orthophosphate formation.

The preponderance of evidence, both experimental and from Quantum Mechanics/Molecular Mechanics (QM/MM) and Electron Valence Bond (EVB) calculations, supports a mechanism in which G protein-catalyzed GTP hydrolysis proceeds through a loose

transition state with dissociative character, as is typical for nucleophilic attack on phospho-monoesters^{76, 77}. As such, a catalytic base to deprotonate the nucleophile would not promote catalysis (see Lassila et al. for a comprehensive discussion⁷⁶). Findings are based for the most part on studies of Ras:Ras-GAP, which, with some caution, may be applied to the intrinsic GTPase activity of G α , in which the Arg_{cat}, that resides in switch I is a built-in component of the active site. Strong evidence for a loose transition state comes from the significant normal kinetic ¹⁸O isotope effect (V/K = 1.02) at the bridging β - γ oxygen atom of the leaving group, and secondary isotope effects in the non-bridging β phosphate oxygens^{78, 79}. These are indicative of a redistribution of negative charge towards the β - γ bridge oxygen and to the non-bridging β phosphate oxygen atoms as well (with a concomitant reduction in their bond orders). The magnitude of this kinetic isotope effect (KIE) suggests a low forward commitment to the formation of this transition state and hence, that it is the rate-limiting step of the reaction. In contrast, KIEs at γ phosphate oxygen atoms are near unity, and hence inconsistent with an associative transition state or phosphoryl intermediate. Time-resolved Infrared and Raman spectroscopy of Ras-GAP catalyzed turnover of caged, ¹⁸O-labeled GTP after photoexcitation, similarly report accumulation of charge in the β phosphate oxygens⁸⁰⁻⁸², and further, vibrational decoupling of the phosphates resulting from their differential interactions with the Ras active site. QM/MM simulations based on the Ras-GAP complex with GDP•MgAlF indicate a metaphosphate (PO₃⁻) intermediate^{83, 84}. The trend in KIE values with respect to the site of ¹⁸O labeling is correctly predicted by this model⁸⁵. Whether an actual metaphosphate intermediate forms is doubtful. Electron Valence Bond calculations and KIE effects appear to support a more concerted reaction with dissociative character⁸⁶. In such a mechanism, to accelerate catalysis, the active site of G α must draw electron density from the bond between the β - γ bridging oxygen and the leaving group, by stabilizing charge at that oxygen and delocalizing charge to the non-bridging oxygen atoms of the β phosphate.

Part of the task of charge redistribution falls to amide groups of the P-loop. For Ras, Maegley et al. saw the amide group of Gly 13 (Glu 43 in G α i1) as a prime candidate for this role, in view of the short hydrogen bond that it forms to the β - γ bridging oxygen of GTP in several Ras structures⁸⁷. Indeed, a short, linear 2.7Å hydrogen bond between the corresponding atoms is observed in the crystal structure of the Ras:Ras-GAP complex⁷⁰. Accordingly, a normal isotope effect is observed for the β - γ bridging oxygen, as well as the Pro-S β oxygen, which accepts hydrogen bonds from P-loop amides at residues 15 and 16, as well as the amine of lysine 16 (Lys 46 in G α i1)⁷⁹. These hydrogen bonds are conserved in the GDP•MgAlF-bound structures of G α i1 and G α t, as well as in the GTP γ S or GppNHp ground states. Thus, there are ample hydrogen bond donors available to stabilize charge on the β -phosphate leaving group. Nevertheless, robust stabilization of charge on the β - γ bridging oxygen requires Arg_{cat}, whether it is supplied by an exogenous GAP, or, as in G α subunits, is resident in switch I. KIE experiments suggest that the Arg_{cat} \rightarrow Ala mutation considerably impairs the GAP activity of NF1⁷⁹ by eliminating the Arg_{cat} contribution to charge stabilization at the pro-S β phosphate oxygen. In heterotrimeric G proteins, mutation of the endogenous Arg_{cat} results in loss of GTPase activity in G α s^{88, 89}. The same residue is the target of cholera toxin ADP ribosylation⁹⁰.

Arg_{cat} exerts its catalytic function at the transition state. As noted above, GTP-analog-bound structures of Gα subunits differ in the disposition of Arg_{cat}. In Gat•GTPγS, Arg_{cat} is hydrogen bonded to the β-γ bridging oxygen; in Gαi•GTPγS and Gαs•GTPγS, it is partially disordered, and in the “auto-inhibited” conformation observed in Gαi1•GppNHP, Arg_{cat} is sequestered from the nucleotide by formation of an ion pair with the side chain of P-loop Glu 43. However, in the GDP•MgAlF complexes of Gαi1, Gαo, Gat, Gαq, Gα12 and Gα13 (some also bound to effector-GAPs), the conformation of Arg_{cat} is invariant, forming in all instances hydrogen bonds to both the bridging oxygen atom and a fluoride substituent of AlF^{14, 45, 48, 50, 52, 69}. In these structures, Gln_{cat} accepts a hydrogen bond from W_{nuc} and donates to a fluoride substituent of AlF (Figure 2c).

Resolution of the loose dissociative transition state is achieved by scission of the bond between Pγ and the β-γ bridging oxygen of the leaving group and formation of a bond from the metaphosphate-like species to the attacking water. This step involves the transfer of a proton from the W_{nuc} to the γ phosphate, yielding GDP and H₂PO₄⁻. Whether concerted with the breakdown of the dissociative transition state or following it, direct transfer of the proton is energetically prohibitive⁸³. A “two-water”⁸⁶ proton transfer trajectory, presumably along existing hydrogen bonds, would afford a lower energy route but would require shuttling the proton through an intermediary donor/acceptor. None of the crystal structures of Gα•GDP•MgAlF complexes reveal a water molecule optimally positioned to shuttle a proton from W_{nuc} to a γ phosphate oxygen. Sondek, et al. proposed such a role for Gln_{cat}, wherein the side chain Oδ abstracts a proton from W_{nuc} while the δ amide donates a proton to the γ phosphate¹⁴. This highly unlikely tautomeric shift, in view of the pKas of the groups involved, could be driven by a highly reactive metaphosphate (PO₃⁻) intermediate⁸³. In any case, the absence, in Ras:Ras-GAP-catalyzed GTP hydrolysis, of a KIE on the γ phosphate oxygen atoms suggests that proton transfer to the γ phosphate is not rate limiting⁷⁹.

Lessons from mutants

Both site-directed mutagenesis and natural sequence variations have provided insight into Gα function. Some outcomes are expected - for example, that mutations of Gln_{cat} and Arg_{cat} result in constitutive activity, unregulated signaling and associations with pituitary and pancreatic cancer^{89, 91–94}. The X-ray structures of Gαi1•GTPγS harboring these mutations, Q204R and R178C, respectively, show no perturbations of the GTP binding site⁶⁹. The presumptive W_{nuc} is observed in the structures of both mutants, as in the structure of wild-type Gαi1•GTPγS, some 3.8Å from the γ phosphate. Thus, neither residue participates significantly in substrate binding, as confirmed by the rates of nucleotide dissociation.

With a turnover rate less than 0.1 min⁻¹ at 30°C, 100-fold slower than Gαi1, Gαz is an exceptionally sluggish GTPase. Gαz harbors threonine and serine residues at positions 41 and 42 of the P-loop, whereas alanine and glycine are found in Gα subunits with typical levels of GTPase activity. Although a modeling experiment suggests that both sequence variations can be easily accommodated in the P-loop, it is possible that, together, they perturb the P-loop amide hydrogen bonds to the GTP β phosphates, and impair the ability of the enzyme to stabilize negative charge at the transition state. Gαq also has a threonine at

position 41 (but retains the canonical glycine at 42) and has moderately weak GTPase activity at 0.8 min^{-1} . Thus, evolutionary forces are able to tune intrinsic $G\alpha$ GTPase activities by P-loop mutations that do not appear to significantly perturb the stereochemistry of the catalytic site.

More surprising are mutations that alter $G\alpha$ conformation or dynamics in a substrate-dependent manner. Seemingly modest mutagenic perturbations of the P-loop and switch II can result in significant alterations in the GTP, Mg^{2+} or $G\beta\gamma$ binding properties of $G\alpha$, and may be manifested in novel conformations that can be trapped in the solid state. In $G\alpha_s$, mutation of Gly 226 to alanine results in a serious signaling defect in which receptor engagement of heterotrimeric Gs fails to liberate $G\alpha_s\cdot\text{GTP}$ and $G\beta\gamma$ ^{95, 96}. Gly 226 is located at the N-terminus of switch II, where its amide group forms a hydrogen bond with a γ phosphate oxygen atom (the equivalent residue in Ras is Gly 60). Because Gly 226 is in van der Waals contact with the P-loop residue Gly 49, substitution with alanine would be expected to introduce a steric clash in that region. Nevertheless, (G226A) $G\alpha_s$ activates adenylyl cyclase. It and its homolog (G203A) $G\alpha_i1$ have nearly normal GTPase activity, but weaker-than-wild-type affinity for Mg^{2+} and $\text{GTP}\gamma\text{S}$ ^{96, 97}.

Surprisingly, an attempt to crystallize the $\text{GTP}\gamma\text{S}:Mg^{2+}$ complex of (G203A) $G\alpha_i1$ instead yielded crystals of the Mg^{2+} -free complex of GDP with inorganic phosphate (Pi): a model of the ternary product complex of GTP hydrolysis⁹⁸ (Figure 2d). Presumably, at the low pH (~ 5.5) at which the complex was crystallized, the relatively unreactive GTP analog was hydrolyzed during the course of crystallization. The position occupied by GDP and its contacts with the P-loop in the G203A mutant are no different from those observed in wild-type $G\alpha_i1$. The phosphate, most likely H_2PO_4^- , is within hydrogen bonding distance of the β phosphate, stabilized by the P-loop lysine and switch II Arg_{cat} . To accommodate Pi, switch II adopts a more regular helical structure at its N-terminus and becomes kinked near its midpoint, affording its movement away from the catalytic site. Meanwhile, the hydrogen bond between the 203 amide nitrogen and the erstwhile γ phosphate is maintained. Thus, due to a substantial change in the secondary structure of switch II, $G\alpha_i1$ adopts a conformation that is complementary to $\text{GDP}\cdot\text{Pi}$. Yet, Pi binds very weakly to $G\alpha_i1\cdot\text{GDP}$ – both to the wild-type and G203A and G42V (see below) mutants – with a K_d of at least 50 mM ⁹⁹. Arguably, by placing steric stress at the N-terminus of switch II A203 stabilized a transitory conformational state, thus trapping the $\text{GDP}\cdot\text{Pi}$ product complex. Precisely the same $\text{GDP}\cdot\text{Pi}$ -bound state of the (A42V) $G\alpha_i1$ mutant can be crystallized⁹⁹. Like its oncogenic G12A counterpart in Ras¹⁰⁰, (A42V) $G\alpha_i1$ has weak GTP hydrolytic activity, with a turnover rate of 0.13 min^{-1} . GTPase activity may be weakened in this mutant due to steric conflict between the Val 42 side chain and $C\beta$ of Gln_{cat} . Accordingly, the steric pressure that induces the reconfiguration of switch II, and affords crystallization of the $\text{GDP}\cdot\text{Pi}$ complex, originates from an increase in side-chain volume at position 42 in the P-loop.

As we have seen, mutations in switch I and switch II have the potential to drastically alter GTPase activity. Mutation of Gly 202 to alanine, perhaps because it forms a hydrophobic cage that restricts the mobility of W_{nuc} , causes a 10-fold increase in the intrinsic GTPase rate of $G\alpha_i1$ ¹⁰¹. The reverse mutation in Ras, in which the corresponding wild-type residue at position 59 is alanine, results in the loss of GTPase activity¹⁰². In the crystal structure of

(A59G)Ras•GppNHp, switch II adopts a conformation that is intermediate between the GTP and GDP-bound states. Unfortunately, it was not possible to crystallize (G202A)Gαi1 as a complex with a GTP analog.

Mutations that trap intermediate states have been found elsewhere near the catalytic site. The switch I residue located two positions N-terminal to Arg_{cat} is variable among the different Gα classes. In Gi-class Gα subunits, this position is occupied by lysine; in the q/11 Gα class, proline is preferred. This substitution has no effect on the conformation of switch I, because the backbone φ/ψ angles at that position are accessible to proline. However, substitution of lysine for proline resulted in an eight-fold loss of GTPase activity¹⁰³, whereas a lysine-to-alanine mutation had no effect. However, the impact of this mutation on conformational change rates was startling.

Increase in intrinsic tryptophan fluorescence is a hallmark of Gα activation^{64, 104} that originates from changes in the solvent accessibility of a tryptophan in switch II upon exchange of GDP for GTP¹⁰⁵. Hence, a convenient way to follow GTP hydrolysis has been to monitor the rate at which tryptophan fluorescence is lost as hydrolysis proceeds¹⁰⁶. Indeed, the rate of the fluorescence transition is nearly identical to that at which GTP is hydrolyzed as measured by generation of radiolabeled Pi¹⁰⁷ or fluorescence quenching of N-methyl-anthranoyl guanine nucleotide derivatives (mGTP)¹⁰⁸. For (K180P)Gαi1, the rate of tryptophan fluorescence decay upon addition of Mg²⁺ to GTP-bound protein exceeded by 60-fold that of Pi or mGDP production. Apparently, switch II began its conformational change before GTP was hydrolyzed, and thus the two events were decoupled. Attempts to crystallize the K180P mutant in the presence of Mg²⁺ and a hydrolysis-resistant GTP analog were not successful, so the structure of the intermediate from which hydrolysis proceeds remains unknown. The structure of the pre-transition state GDP•MgAlF complex indicated destabilization of the Mg²⁺ binding site, with switch I constrained by the proline substitution to a conformation similar to the GTP-bound state. The behavior of this mutant suggests the possibility that catalytic pre-organization may involve long-range structural changes that preserve the coupling between GTP hydrolysis and conformational changes in switch II.

Convergent mechanisms of Gα GTPase activating proteins

In the mid-1990s, experiments with yeast and nematodes lead to the discovery of “Regulators of G protein Signaling” (RGS)¹⁰⁹, which were ultimately found to function as GTPase activating proteins (GAPs) for Gα, acting catalytically to increase the rate of Gα-catalyzed GTP hydrolysis by up to 100-fold *in vitro*¹¹⁰. GAP activity in these proteins is conveyed by a ~120 residue α-helical domain. RGS proteins play complex, integrative roles in cell signaling, acting as “kinetic scaffolds” in conjunction with G protein heterotrimers and GPCRs to maintain high signaling throughput by coupling Gα activation to GTP hydrolysis^{111–113}. Much has been learned about the basis of Gα class specificity exhibited by members of the four major families of RGS GAPs, and their complex roles in cell signaling⁴⁰. Here we focus on the mechanism by which they accelerate GTP hydrolysis and the remarkable functional convergence of RGS GAPs with certain G protein effectors, which also function as GAPs. Among these are isoforms of PLC-β^{55, 71} and p115RhoGEF, one of a family of Gα12/13-regulated guanine nucleotide exchange factors for the Rho GTPases¹¹⁴.

When co-localized at the plasma membranes with GPCRs and $G\beta\gamma$, these too, kinetically couple G-protein activation and de-activation, maintaining a high steady-state level of effector activation while agonists are present. This is possible because $G\alpha$ GAPs and effectors occupy distinct and non-overlapping binding sites on $G\alpha$ ²⁵. In reconstituted vesicles containing $G\alpha$, $G\beta\gamma$, a GPCR and the appropriate RGS protein or effector-GAP, GTP turnover rates can be 1000-fold higher than intrinsic GTPase rates¹¹². The maximal catalytic efficiency for $G\alpha$ •GTP as a GAP substrate is $\sim 10^8 \text{ M}^{-1}\text{s}^{-1}$, with K_M values ranging from ~ 2 to 600 nM for various RGS proteins, and in the nanomolar range for PLC- $\beta 1$ ^{55, 112} and p115RhoGEF¹¹⁵. The effect of GAPs on the K_M for GTP at the catalytic site of $G\alpha$ has not been determined, hence we cannot know how the catalytic efficiency of $G\alpha$ itself is affected.

RGS GAPs exhibit high affinity for the pre-transition state of $G\alpha$ as modeled by the complex of $G\alpha$ •GDP•MgAlF¹¹⁶. The crystal structure of $G\alpha i 1$ •GDP•MgAlF:RGS4 is the prototype for RGS domain-bound $G\alpha$ complexes that have been subsequently determined^{45, 117–120} and which currently represent three of the four subfamilies of RGS GAPs bound to α subunits of the *i* ($G\alpha t$, $G\alpha i 1$, $G\alpha i 3$) and *q* ($G\alpha q$) classes. As yet, no RGS GAP that recognizes $G\alpha s$ has been discovered, and it appears that the $t_{1/2}$ for adenylyl cyclase activation is similar to that of the intrinsic rate of $G\alpha s$ -catalyzed GTP hydrolysis⁵⁹. In all of these complexes, we find that RGS, unlike small G protein GAPs that provide Arg_{cat} , does not contribute residues that appear to have a direct catalytic function. Rather, RGS sterically restrains the conformation of switch I and switch II, and in particular, Gln_{cat} and Arg_{cat} , to stabilize the pre-transition state conformation of $G\alpha$ (Figure 4a). Accordingly, RGS domains form contacts with all three switch regions (I-III), and some engage the helical domain (*viz.* RGS2 and $G\alpha q$ ¹²⁰). Most RGS domains provide a conserved asparagine as a hydrogen bonding partner for Gln_{cat} , thereby stabilizing its conformation in the pre-transition state. However mutagenesis studies, reviewed by Ross and Wilkie⁵⁹, and structures that have been determined so far, suggest that considerable variation is tolerated at the RGS: $G\alpha$ interface. Stabilization of Gln_{cat} is crucial. RGS4 cannot restore GTPase activity to (Q204L) $G\alpha i 1$ ¹²¹ but can rescue the GTPase activity of the Arg_{cat} mutant R178C, although not to levels exhibited by wildtype $G\alpha$. The active site structure of the (R183C) $G\alpha q$ •GDP•MgAlF bound to RGS2 is virtually identical to that of RGS domains bound to wild-type $G\alpha$ subunits¹²⁰. Thus, the incremental stabilization of charge at the β - γ leaving group oxygen is not essential if Gln_{cat} can be conformationally stabilized to effect catalysis.

The GAP activity of PLC- $\beta 3$ results from the interaction of an extended loop between the third and fourth EF hand domains with the switch I and switch II regions of $G\alpha q$ ⁴⁸. At the contact site, PLC- $\beta 3$ residue Asn 260 is juxtaposed to Gln_{cat} in much the same fashion as the essential Asn residue provided by RGS domains (Figure 4b). Here, too, it appears that PLC- β exerts GAP activity by stabilizing the pre-transition state of Gln_{cat} . As an effector, PLC- β also has high affinity for the GTP-bound forms of $G\alpha q$ and accordingly, interactions between the two molecules involve an extensive interface that involve switch I and II as well as the trough between switch II and $\alpha 3$, which is typically reserved for effector binding.

Gα12/13-activated p115RhoGEF affords a 60-fold stimulation of the GTPase activity of Gα13, and a more modest 6-fold acceleration of that for Gα12¹¹⁵. Although p115RhoGEF and its homologs possess RGS-homology (RH or rgRGS) domains, these are not involved in GAP activity. The structure of the complex between the rgRGS domain and a Gα13/Gα11 chimera revealed that the RGS-like domain binds to Gα13/I in the manner of an effector, with extensive contacts at the switch II - α3 interface, rather than as a GAP⁴⁹ (Figure 3c). GAP activity was instead conferred by a 20-residue peptide segment (named βN-αN) directly N-terminal to the RGS-like domain (Figures 3c, 4c). The peptide is folded into an antiparallel β-α hairpin. The β segment contains a short hydrophobic sequence that docks against the helical domain of Gα13; a mainchain carbonyl oxygen within this sequence is engaged in a hydrogen bond with an arginine residue in switch III⁵². The α- helical segment harbors a highly acidic sequence interrupted by a phenylalanine residue (EDEDFE). These residues are critical for GAP activity. The first glutamate residue in this acidic region stabilizes Arg_{cat}, and the phenylalanine side chain is positioned analogously to the conserved Asn residue of RGS domains, where it sterically restrains Gln_{cat} in its pre-transition state conformation. Mutagenesis of either residue to alanine abolishes GAP activity. The related PDZRhoGEF retains the ability to bind GTPγS-activated Gα12 and Gα13, but has no GAP activity, even though it has affinity for GDP•MgAIF-bound Gα13¹²². The acidic motif of PDZRhoGEF contains a single deletion in the acidic motif and a tyrosine replaces the phenylalanine (EEDY). Crystal structures show that the misalignment between the shortened acidic motif results in weakened interactions with switch I, reorientation of the tyrosyl residue relative to the position of phenylalanine at the corresponding site in p115RhoGEF, and a loss of order throughout the acidic region⁵².

RGS GAPs, PLC-β and 115RhoGEF, though disparate in structure and amino acid sequence, have converged on roughly the same mechanism for GAP activation. Each stabilizes the pre-transition state conformation of Gα by stabilizing catalytic conformations of Arg_{cat} and, particularly, Gln_{cat}. Overall binding energy derives from interactions with switches I-III, to differing extents with the Gα helical domain, and in the case of effector-GAPs, with Gα effector-binding regions that, at minimum, include switch II and α3. Unlike Ras-family GAPs, Gα GAPs do not participate in the chemistry of GTP hydrolysis. More generally, the structural and kinetic data obtained from Gα mutants suggest that protein dynamics may ultimately determine the rate of GTP hydrolysis by controlling the density of conformational states from which the active site of Gα can access the pre-transition state along a low activation energy pathway. Gα GAPs accelerate hydrolysis by constraining an otherwise mobile switch II, particularly Gln_{cat}, forcing it to orient the water nucleophile for in-line attack and stabilizing Arg_{cat} through a hydrogen bonding network that includes the γ phosphate. In this way Gα GAPs both promote the pre-organization of the catalytic site and indirectly assist in stabilizing charge at the βγ bridging oxygen – thus lowering the activation energy barrier to release of the leaving group.

Functional consequences of GTP hydrolysis

While GTP hydrolysis modestly diminishes the affinity of Gαi for effectors, it markedly increases affinity for Gβγ¹⁰. Gαi•GDP forms a high affinity, nanomolar K_d complex with Gβγ that sequesters both signaling molecules in an inactive state at the plasma membrane.

The release of interactions between the γ -phosphate and the N-terminus of switch II allows the latter to refold, affording new interactions at the $G\beta\gamma$ interface^{18–20}. In the heterotrimer, the $\beta 2$ strand and the N-terminus of switch II – an extension of $\beta 3$ – are knit together as in a parallel, hydrogen-bonded network extending to Thr 181 in switch I and Ala 203 in switch II (residues 201 – 204 adopt an unusual 2⁷ helical turn). In this configuration, strands $\beta 1$ together with $\beta 3$ and switch II form a platform for the $G\beta$ subunit. Major switch II participants in this interaction are Lys 210 and Gln_{cat}, which now plays a structural rather than a catalytic role. Further along in Switch II, the side chain of Lys 210 is buried in the interface with $G\beta$. The importance of these residues to the affinity of the $G\alpha:G\beta$ interaction has been noted in computational modeling studies¹²³.

Reactivation of $G\alpha$: exchange of GDP for GTP

It is remarkable that a single phosphate moiety at the γ position of GTP is sufficient to effect major rearrangements in switch I and II that liberate both $G\alpha i 1$ and $G\beta\gamma$ to fulfil their respective roles in GPCR-actuated signaling. In cells, the preponderance of membrane-associated $G\alpha \cdot GDP$ is bound in a complex with $G\beta\gamma$. The conformational changes within switch I and II that are necessary to accommodate GTP cannot occur within the heterotrimer, which binds to GDP with 100-fold greater affinity than free $G\alpha$ subunits¹⁰, and within which GDP is inaccessible to solvent^{18, 20}. Rather, GDP must first be released by engagement of the heterotrimer with an agonist-activated GPCR. The extensive conformational changes that result in the ejection of GDP are exemplified in the crystal structure of heterotrimeric Gs bound to the $\beta 2$ adrenergic receptor²¹. This structure, together with studies using structure-based mutagenesis^{124–127}, site-directed spin-labeling^{128–130}, molecular dynamics^{131–133} and other computational approaches¹³⁴ have arrived at a consistent picture of the receptor-induced conformational transitions that compel GDP release. These and seminal papers reviewed elsewhere (see ^{135, 136}) show that GPCRs engage the C-terminus of $G\alpha$ ^{137, 138}, causing it to rotate slightly and translate with respect to the body of the Ras domain. This key perturbation induces conformational changes in the $\alpha 5$ - $\beta 6$ loop at the purine binding site, disrupts interactions with the $\alpha 1$ helix and succeeding P-loop, and destabilizes the nucleotide binding site and contacts between the Ras and helical domains, leading to their separation and facilitating egress of GDP. The cytosolic non-receptor nucleotide exchange factor Ric-8A induces similar and possibly more extensive conformational changes in the structure of $G\alpha i 1$ ¹³⁹.

While the interface between $G\alpha$ s switch II and $G\beta\gamma$ is largely intact in the complex with the $\beta 2$ receptor, this interaction is weakened with the disordering of switch I. The P-loop adopts an open conformation, ready to receive the β and γ phosphates of GTP and, with these moieties, to coordinate a magnesium ion¹²³. Awaiting further exploration are the coupled conformational pathways by which the P-loop, switch II and $\beta 5$ - $\alpha 5$ refold around GTP, and thus escape from the complex with $G\beta\gamma$ and the receptor. In aggregate, these rearrangements would eliminate the switch II interface with $G\beta$, and disrupt that between the receptor and $\alpha 5$.

Conclusions

In the presence of magnesium ion, GTP binds with nanomolar affinity to the α subunits of heterotrimeric G proteins. This extraordinarily high binding energy is used to restrain and stabilize the conformation of otherwise highly dynamic $G\alpha$ switches I and II. The conformation in which these two structural elements are held is highly complementary to the surfaces of $G\alpha$ effectors, but incompatible with the $G\alpha$ binding site on $G\beta\gamma$. Upon GTP hydrolysis, the energy of these conformational restraints is dissipated and the two switch segments, particularly switch II, become flexible. The GDP-bound state of $G\alpha$ is easily remodeled for binding to $G\beta\gamma$. Both signal transducers – $G\alpha$ and $G\beta\gamma$ – are thereby locked into a nanomolar-affinity complex that can be released only by the catalytic action of agonist-activated G protein-coupled receptors, which allows GTP to disrupt the $G\alpha$: $G\beta\gamma$ interface and that with the receptor itself.

The mechanism by which $G\alpha$ hydrolyzes GTP is likely the same as that used by Ras, with the important difference that $G\alpha$ possesses a catalytic arginine residue that is absent in Ras, and must be supplied by an exogenous GAP. This provides $G\alpha$ with about three orders of magnitude in rate enhancement relative to Ras with respect to intrinsic GTPase activity. The intrinsic GTPase rates of different classes of $G\alpha$ range from $\sim 0.1 \text{ min}^{-1}$ to 4 min^{-1} at $\sim 20 \text{ }^\circ\text{C}$. The differences are likely due in large part to the amino acid sequence of the P-loop, resulting in greater or lesser efficiency in stabilizing charge at the leaving group. Catalytic site pre-organization presents a significant barrier to catalysis possibly due to the richness of non-catalytic states that are accessible to critical residues in the active site of $G\alpha$. Some of these states, exemplified by the apparently “anticatalytic” conformation exhibited in the structure of $G\alpha_{i1}\cdot\text{GppNHp}$ (Figure 2b), may actually impede catalytic action. $G\alpha$ GAPs act by restricting the conformational freedom of $G\alpha$ active site residues, particularly Gln_{cat} and Arg_{cat} and enforcing upon them a conformation that is complementary to the transition state for GTP hydrolysis. Gln_{cat} in particular, appears to orient and stabilize the γ phosphate and the water nucleophile for an in-line attack. The transition state is probably loose with dissociative character, and phosphoryl transfer may be concerted. Experimental, structural and computational data suggest that electron density from the γ phosphate shifts to the β - γ bridge oxygen and is redistributed to the β non-bridging oxygens. $G\alpha$, and more effectively $G\alpha$:GAP, catalyzes GTP hydrolysis by promoting this charge redistribution. Along the reaction pathway, possibly in concert with the collapse of the loose transition state, a proton is shuttled from the water nucleophile to the γ phosphate, affording H_2PO_4^- . An ordered water molecule would be an ideal candidate to serve as a shuttle, but it is also possible that Gln_{cat} might act in this capacity. There is still a need for conclusive answers to several questions: does a metaphosphate intermediate occur in the reaction trajectory, or is the reaction concerted, with a loose-transition state? What is the mechanism of proton transfer to the γ phosphate? What, precisely is the role of Gln_{cat} ? Importantly, why, given the relatively small structural differences between the $G\alpha\cdot\text{GTP}$ “Michaelis” complex and the pre-transition state as modeled by the $\text{GDP}\cdot\text{MgAlF}$ complex, is the activation energy barrier to GTP hydrolysis so high?

It appears that $G\alpha$ GAPs have arisen independently on several occasions during the evolution of $G\alpha$ -regulated signal transduction networks. Incorporation of GAP activity into

effectors affords exquisite regulation of GTPase kinetics and effector activation. Co-localization with GPCRs provides additional avenues for steady-state control of G protein signaling. RGS GAPs are structurally well conserved, but several have acquired signaling functions unrelated to GAP activity. For example, the RGS domains present in members of the RGS-RhoGEF family engage G α in the manner of effectors, whereas GAP activity is conveyed by a short β - α peptide motif. Although they are structurally dissimilar, RGS GAPs and the GAP-domains of RGS-RhoGEFs and PLC- β converge on a common mechanism of action, which is to stabilize the pre-transition state for G α -catalyzed GTP hydrolysis, acting primarily on the conformation of Arg_{cat} and Gln_{cat}. Arguably, we have a fairly clear understanding of the reaction kinetics and structural transformations involving G α subunits in the context of the canonical GTPase cycle of activation, effector regulation and signal termination. Considerably less well understood are G α class-specific modes of signal integration - processes that may involve transient, often membrane-associated, multiprotein complexes that assemble at the plasma membrane and interact with other regulators. Remarkably, many of the proteins that support such signaling agendas harbor RGS domain modules, for example, RGS7, RGS14 and RGS-RhoGEFs¹⁴⁰. Unraveling the complex web of G protein regulatory interactions involving these and other signal transducers is our present task.

Acknowledgments

Research conducted in the author's laboratory has been supported by NIH grants R01-DK046371 and R01-GM105993.

Literature Citations

1. Cassel D, Selinger Z. *Biochim Biophys Acta*. 1976; 452:538–551. [PubMed: 188466]
2. Pfeuffer T, Helmreich EJ. *J Biol Chem*. 1975; 250:867–876. [PubMed: 1120776]
3. Ross EM, Howlett AC, Ferguson KM, Gilman AG. *J Biol Chem*. 1978; 253:6401–6412. [PubMed: 210183]
4. Pfeuffer T. *J Biol Chem*. 1977; 252:7224–7234. [PubMed: 903360]
5. Gilman AG. *Annual Reviews in Biochemistry*. 1987; 56:615–649.
6. Stryer L. *Annual review of neuroscience*. 1986; 9:87–119.
7. Brandt DR, Ross EM. *J Biol Chem*. 1985; 260:266–272. [PubMed: 2981206]
8. Ferguson KM, Higashijima T, Smigel MD, Gilman AG. *J Biol Chem*. 1986; 261:7393–7399. [PubMed: 3086311]
9. Higashijima T, Ferguson KM, Smigel MD, Gilman AG. *J Biol Chem*. 1987; 262:757–761. [PubMed: 3027067]
10. Higashijima T, Ferguson KM, Sternweis PC, Smigel MD, Gilman AG. *J Biol Chem*. 1987; 262:762–766. [PubMed: 3100519]
11. Fung BK. *J Biol Chem*. 1983; 258:10495–10502. [PubMed: 6136509]
12. Sternweis PC, Northup JK, Smigel MD, Gilman AG. *J Biol Chem*. 1981; 256:11517–11526. [PubMed: 6271754]
13. Lambright DG, Noel JP, Hamm HE, Sigler PB. *Nature*. 1994; 369:621–628. [PubMed: 8208289]
14. Sondak J, Lambright DG, Noel JP, Hamm HE, Sigler PB. *Nature*. 1994; 372:276–279. [PubMed: 7969474]
15. Noel JP, Hamm HE, Sigler PB. *Nature*. 1993; 366:654–663. [PubMed: 8259210]
16. Coleman DE, Berghuis AM, Lee E, Linder ME, Gilman AG, Sprang SR. *Science*. 1994; 265:1405–1412. [PubMed: 8073283]

17. Mixon MB, Lee E, Coleman DE, Berghuis AM, Gilman AG, Sprang SR. *Science*. 1995; 270:954–960. [PubMed: 7481799]
18. Wall MA, Coleman DE, Lee E, Iniguez-Lluhi JA, Posner BA, Gilman AG, Sprang SR. *Cell*. 1995; 83:1047–1058. [PubMed: 8521505]
19. Wall MA, Posner BA, Sprang SR. *Structure*. 1998; 6:1169–1183. [PubMed: 9753695]
20. Lambright DG, Sondek J, Bohm A, Skiba NP, Hamm H, Sigler PB. *Nature*. 1996; 379:311–319. [PubMed: 8552184]
21. Rasmussen SG, DeVree BT, Zou Y, Kruse AC, Chung KY, Kobilka TS, Thian FS, Chae PS, Pardon E, Calinski D, Mathiesen JM, Shah ST, Lyons JA, Caffrey M, Gellman SH, Steyaert J, Skinotitis G, Weis WI, Sunahara RK, Kobilka BK. *Nature*. 2011; 477:549–555. [PubMed: 21772288]
22. Sprang SR. *Annual review of biochemistry*. 1997; 66:639–678.
23. Vetter IR, Wittinghofer A. *Science*. 2001; 294:1299–1304. [PubMed: 11701921]
24. Coleman DE, Sprang SR. *Biochemistry*. 1998; 37:14376–14385. [PubMed: 9772163]
25. Sprang SR, Chen Z, Du X. *Advances in protein chemistry*. 2007; 74:1–65. [PubMed: 17854654]
26. Dohlman HG, Jones JC. *Sci Signal*. 2012; 5:re2. [PubMed: 22649098]
27. Pierce KL, Premont RT, Lefkowitz RJ. *Nat Rev Mol Cell Biol*. 2002; 3:639–650. [PubMed: 12209124]
28. Rosenbaum DM, Rasmussen SG, Kobilka BK. *Nature*. 2009; 459:356–363. [PubMed: 19458711]
29. Sternweis PC. *Curr Opin Cell Biol*. 1994; 6:198–203. [PubMed: 8024810]
30. Clapham DE, Neer EJ. *Annu Rev Pharmacol Toxicol*. 1997; 37:167–203. [PubMed: 9131251]
31. Gautam N, Downes GB, Yan K, Kisselev O. *Cell Signal*. 1998; 10:447–455. [PubMed: 9754712]
32. Wedegaertner PB, Wilson PT, Bourne HR. *J Biol Chem*. 1995; 270:503–506. [PubMed: 7822269]
33. Smotrys JE, Linder ME. *Annual review of biochemistry*. 2004; 73:559–587.
34. Linder ME, Pang IH, Duronio RJ, Gordon JI, Sternweis PC, Gilman AG. *J Biol Chem*. 1991; 266:4654–4659. [PubMed: 1900297]
35. Tall GG, Krumins AM, Gilman AG. *J Biol Chem*. 2003; 278:8356–8362. [PubMed: 12509430]
36. Preininger AM, Kaya AI, Gilbert JA 3rd, Busenlehner LS, Armstrong RN, Hamm HE. *Biochemistry*. 2012; 51:1911–1924. [PubMed: 22329346]
37. Gilman AG. *Ann Rev Biochem*. 1987; 56:615–649. [PubMed: 3113327]
38. Cabrera-Vera TM, Vanhauwe J, Thomas TO, Medkova M, Preininger A, Mazzoni MR, Hamm HE. *Endocr Rev*. 2003; 24:765–781. [PubMed: 14671004]
39. Oldham WM, Hamm HE. *Q Rev Biophys*. 2006; 39:117–166. [PubMed: 16923326]
40. Hubbard KB, Hepler JR. *Cell Signal*. 2006; 18:135–150. [PubMed: 16182515]
41. Aittaleb M, Boguth CA, Tesmer JJ. *Mol Pharmacol*. 2010; 77:111–125. [PubMed: 19880753]
42. Bunemann M, Frank M, Lohse MJ. *Proc Natl Acad Sci U S A*. 2003; 100:16077–16082. [PubMed: 14673086]
43. Frank M, Thumer L, Lohse MJ, Bunemann M. *J Biol Chem*. 2005; 280:24584–24590. [PubMed: 15866880]
44. Tesmer JJG, Sunahara RK, Gilman AG, Sprang SR. *Science*. 1997; 278:1907–1916. [PubMed: 9417641]
45. Slep KC, Kercher MA, He W, Cowan CW, Wensel TG, Sigler PB. *Nature*. 2001; 409:1071–1077. [PubMed: 11234020]
46. Tesmer VM, Kawano T, Shankaranarayanan A, Kozasa T, Tesmer JJ. *Science*. 2005; 310:1686–1690. [PubMed: 16339447]
47. Lyon AM, Tesmer VM, Dhamsania VD, Thal DM, Gutierrez J, Chowdhury S, Suddala KC, Northup JK, Tesmer JJ. *Nat Struct Mol Biol*. 2011; 18:999–1005. [PubMed: 21822282]
48. Waldo GL, Ricks TK, Hicks SN, Cheever ML, Kawano T, Tsuboi K, Wang X, Montell C, Kozasa T, Sondek J, Harden TK. *Science*. 2010; 330:974–980. [PubMed: 20966218]
49. Chen Z, Singer WD, Sternweis PC, Sprang SR. *Nat Struct Mol Biol*. 2005; 12:191–197. [PubMed: 15665872]

50. Kreutz B, Yau DM, Nance MR, Tanabe S, Tesmer JJ, Kozasa T. *Biochemistry*. 2006; 45:167–174. [PubMed: 16388592]
51. Sunahara RK, Dessauer CW, Whisnant RE, Kleuss C, Gilman AG. *J Biol Chem*. 1997; 272:22265–22271. [PubMed: 9268375]
52. Chen Z, Singer WD, Danesh SM, Sternweis PC, Sprang SR. *Structure*. 2008; 16:1532–1543. [PubMed: 18940608]
53. Sunahara RK, Tesmer JJG, Gilman AG, Sprang SR. *Science*. 1997; 278:1943–1947. [PubMed: 9395396]
54. Van Eps N, Oldham WM, Hamm HE, Hubbell WL. *Proc Natl Acad Sci U S A*. 2006; 103:16194–16199. [PubMed: 17053066]
55. Berstein G, Blank JL, Jhon D-Y, Exton JH, Rhee SG, Ross EM. *Cell*. 1992; 70:411–418. [PubMed: 1322796]
56. Casey PJ, Fong HK, Simon MI, Gilman AG. *J Biol Chem*. 1990; 265:2383–2390. [PubMed: 2105321]
57. Bar-Even A, Noor E, Savir Y, Liebermeister W, Davidi D, Tawfik DS, Milo R. *Biochemistry*. 2011; 50:4402–4410. [PubMed: 21506553]
58. Traut TW. *Mol Cell Biochem*. 1994; 140:1–22. [PubMed: 7877593]
59. Ross EM, Wilkie TM. *Annual review of biochemistry*. 2000; 69:795–827.
60. Sutherland EW, Rall TW, Menon T. *J Biol Chem*. 1962; 237:1220–1227. [PubMed: 13918525]
61. Ross EM, Gilman AG. *J Biol Chem*. 1977; 252:6966–6969. [PubMed: 903346]
62. Northup J, Sternweis P, Smigel M, Schleifer L, Ross E, Gilman A. *Proc Natl Acad Sci U S A*. 1980; 77:6516–6520. [PubMed: 6935665]
63. Sternweis PC, Gilman AG. *Proc Natl Acad Sci U S A*. 1982; 79:4888–4891. [PubMed: 6289322]
64. Higashijima T, Ferguson KM, Sternweis PC, Ross EM, Smigel MD, Gilman AG. *J Biol Chem*. 1987; 262:752–756. [PubMed: 3100518]
65. Bigay J, Deterre P, Pfister C, Chabre M. *FEBS Lett*. 1985; 191:181–185. [PubMed: 3863758]
66. Higashijima T, Graziano MP, Suga H, Kainosho M, Gilman AG. *J Biol Chem*. 1991; 266:3396–3401. [PubMed: 1899863]
67. Antonny B, Chabre M. *J Biol Chem*. 1992; 267:6710–6718. [PubMed: 1551879]
68. Antonny B, Sukumar M, Bigay J, Chabre M, Higashijima T. *J Biol Chem*. 1993; 268:2393–2402. [PubMed: 8381408]
69. Coleman DE, Berghuis AM, Lee E, Linder ME, Gilman AG, Sprang SR. *Science*. 1994; 265:1405–1412. [PubMed: 8073283]
70. Scheffzek K, Ahmadian MR, Kabsch W, Wiesmüller L, Lautwein A, Schmitz F, Wittinghofer A. *Science*. 1997; 277:333–338. [PubMed: 9219684]
71. Biddlecome GH, Berstein G, Ross EM. *J Biol Chem*. 1996; 271:7999–8007. [PubMed: 8626481]
72. Mittal R, Ahmadian MH, Goody RS, Wittinghofer A. *Science*. 1996; 273:115–117. [PubMed: 8658179]
73. Coleman DE, Sprang SR. *J Biol Chem*. 1999; 274:16669–16672. [PubMed: 10358003]
74. Glennon TM, Villa J, Warshel A. *Biochemistry*. 2000; 39:9641–9651. [PubMed: 10933780]
75. Shurki A, Warshel A. *Proteins*. 2004; 55:1–10. [PubMed: 14997535]
76. Lassila JK, Zalatan JG, Herschlag D. *Annual review of biochemistry*. 2011; 80:669–702.
77. Admiraal SJ, Herschlag D. *Chemistry and Biology*. 1995; 2:729–739. [PubMed: 9383480]
78. Du X, Black GE, Lecchi P, Abramson FP, Sprang SR. *Proc Natl Acad Sci U S A*. 2004; 101:8858–8863. [PubMed: 15178760]
79. Du X, Sprang SR. *Biochemistry*. 2009; 48:4538–4547. [PubMed: 19610677]
80. Allin C, Ahmadian MR, Wittinghofer A, Gerwert K. *Proc Natl Acad Sci U S A*. 2001; 98:7754–7759. [PubMed: 11438727]
81. Allin C, Gerwert K. *Biochemistry*. 2001; 40:3037–3046. [PubMed: 11258917]
82. Cepus V, Scheidig AJ, Goody RS, Gerwert K. *Biochemistry*. 1998; 37:10263–10271. [PubMed: 9665734]

83. Grigorenko BL, Nemukhin AV, Shadrina MS, Topol IA, Burt SK. *Proteins*. 2007; 66:456–466. [PubMed: 17094109]
84. Grigorenko BL, Nemukhin AV, Topol IA, Cachau RE, Burt SK. *Proteins*. 2005; 60:495–503. [PubMed: 15906320]
85. Nemukhin AV, Shadrina MS, Grigorenko BL, Du X. *Biochemistry Biokhimiia*. 2009; 74:1044–1048. [PubMed: 19916916]
86. B RP, Plotnikov NV, Lameira J, Warshel A. *Proc Natl Acad Sci U S A*. 2013; 110:20509–20514. [PubMed: 24282301]
87. Maegley KA, Admiraal SJ, Herschlag D. *Proc Natl Acad Sci U S A*. 1996; 93:8160–8166. [PubMed: 8710841]
88. Freissmuth M, Gilman AG. *J Biol Chem*. 1989; 264:21907–21914. [PubMed: 2557345]
89. Landis CA, Masters SB, Spada A, Pace AM, Bourne HR, Vallar L. *Nature*. 1989; 340:692–696. [PubMed: 2549426]
90. Van Dop C, Tsubokawa M, Bourne H, Ramachandran J. *J Biol Chem*. 1984; 259:696–698. [PubMed: 6582062]
91. Graziano MP, Gilman AG. *J Biol Chem*. 1989; 264:15475–15482. [PubMed: 2549065]
92. Landis CA, Masters SB, Spada A, Pace AM, Bourne HR, Vallar L. *Nature*. 1989; 340:692–696. [PubMed: 2549426]
93. Lyons J, Landis CA, Harsh G, Vallar L, Grünewald K, Feichtinger H, Duh Q-Y, Clark OH, Kawasaki E, Bourne HR, McCormick F. *Science*. 1990; 249:655–659. [PubMed: 2116665]
94. O'Hayre M, Vazquez-Prado J, Kufareva I, Stawiski EW, Handel TM, Seshagiri S, Gutkind JS. *Nature reviews Cancer*. 2013; 13:412–424. [PubMed: 23640210]
95. Miller RT, Masters SB, Sullivan KA, Beiderman B, Bourne HR. *Nature*. 1988; 334:712–715. [PubMed: 3137475]
96. Lee E, Taussig R, Gilman A. *J Biol Chem*. 1992; 267:1212–1218. [PubMed: 1730644]
97. Berghuis AM, Lee E, Raw AS, Gilman AG, Sprang SR. *Structure*. 1996; 4:1277–1290. [PubMed: 8939752]
98. Mixon MB, Lee E, Coleman DE, Berghuis AM, Gilman AG, Sprang SR. *Science*. 1995; 270:954–960. [PubMed: 7481799]
99. Raw AS, Coleman DE, Gilman AG, Sprang SR. *Biochemistry*. 1997; 36:15660–15669. [PubMed: 9398294]
100. Barbacid M. *Ann Rev Biochem*. 1987; 56:779–827. [PubMed: 3304147]
101. Thomas CJ, Du X, Li P, Wang Y, Ross EM, Sprang SR. *Proc Natl Acad Sci U S A*. 2004; 101:7560–7565. [PubMed: 15128951]
102. Hall BE, Bar-Sagi D, Nassar N. *Proc Natl Acad Sci U S A*. 2002; 99:12138–12142. [PubMed: 12213964]
103. Posner BA, Mukhopadhyay S, Tesmer JJ, Gilman AG, Ross EM. *Biochemistry*. 1999; 38:7773–7779. [PubMed: 10387017]
104. Phillips WJ, Cerione RA. *J Biol Chem*. 1986; 263:15498–15505.
105. Faurobert E, Otto-Bruc A, Chardin P, Chabre M. *Journal of the European Molecular Biology Organization*. 1993; 12:4191–4198.
106. Guy PM, Koland JG, Cerione RA. *Biochemistry*. 1990; 29:6954–6964. [PubMed: 2223753]
107. Lee E, Linder M, Gilman A. *Methods Enzymol*. 1994; 237:146–164. [PubMed: 7934993]
108. Remmers AE, Posner R, Neubig RR. *J Biol Chem*. 1994; 269:13771–13778. [PubMed: 8188654]
109. Dohlman HG. *Progress in molecular biology and translational science*. 2009; 86:1–14. [PubMed: 20374711]
110. Chidiac P, Ross EM. *J Biol Chem*. 1999; 274:19639–19643. [PubMed: 10391901]
111. Turcotte M, Tang W, Ross EM. *PLoS computational biology*. 2008; 4:e1000148. [PubMed: 18716678]
112. Mukhopadhyay S, Ross EM. *Proc Natl Acad Sci U S A*. 1999; 96:9539–9544. [PubMed: 10449728]
113. Ross EM. *Curr Biol*. 2008; 18:R777–R783. [PubMed: 18786383]

114. Sternweis PC, Carter AM, Chen Z, Danesh SM, Hsiung YF, Singer WD. *Advances in protein chemistry*. 2007; 74:189–228. [PubMed: 17854659]
115. Kozasa T, Jiang X, Hart MJ, Sternweis PM, Singer WD, Gilman AG, Bollag G, Sternweis PC. *Science*. 1998; 280:2109–2111. [PubMed: 9641915]
116. Berman DM, Kozasa T, Gilman AG. *J Biol Chem*. 1996; 271:27209–27212. [PubMed: 8910288]
117. Tesmer JJ, Berman DM, Gilman AG, Sprang SR. *Cell*. 1997; 89:251–261. [PubMed: 9108480]
118. Soundararajan M, Willard FS, Kimple AJ, Turnbull AP, Ball LJ, Schoch GA, Gileadi C, Fedorov OY, Dowler EF, Higman VA, Hutsell SQ, Sundstrom M, Doyle DA, Siderovski DP. *Proc Natl Acad Sci U S A*. 2008; 105:6457–6462. [PubMed: 18434541]
119. Slep KC, Kercher MA, Wieland T, Chen CK, Simon MI, Sigler PB. *Proc Natl Acad Sci U S A*. 2008; 105:6243–6248. [PubMed: 18434540]
120. Nance MR, Kreutz B, Tesmer VM, Sterne-Marr R, Kozasa T, Tesmer JJ. *Structure*. 2013; 21:438–448. [PubMed: 23434405]
121. Berman DM, Wilkie TM, Gilman AG. *Cell*. 1996; 86:445–452. [PubMed: 8756726]
122. Wells CD, Liu MY, Jackson M, Gutowski S, Sternweis PM, Rothstein JD, Kozasa T, Sternweis PC. *J Biol Chem*. 2002; 277:1174–1181. [PubMed: 11698392]
123. Khafizov K, Lattanzi G, Carloni P. *Proteins*. 2009; 75:919–930. [PubMed: 19089952]
124. Marin EP, Krishna AG, Sakmar TP. *J Biol Chem*. 2001; 276:27400–27405. [PubMed: 11356823]
125. Kaya AI, Lokits AD, Gilbert JA, Iverson TM, Meiler J, Hamm HE. *J Biol Chem*. 2014; 289:24475–24487. [PubMed: 25037222]
126. Sun D, Flock T, Deupi X, Maeda S, Matkovic M, Mendieta S, Mayer D, Dawson RJ, Schertler GF, Babu MM, Veprintsev DB. *Nat Struct Mol Biol*. 2015; 22:686–694. [PubMed: 26258638]
127. Posner BA, Mixon MB, Wall MA, Sprang SR, Gilman AG. *J Biol Chem*. 1998; 273:21752–21758. [PubMed: 9705312]
128. Oldham WM, Van Eps N, Preininger AM, Hubbell WL, Hamm HE. *Nat Struct Mol Biol*. 2006; 13:772–777. [PubMed: 16892066]
129. Oldham WM, Van Eps N, Preininger AM, Hubbell WL, Hamm HE. *Proc Natl Acad Sci U S A*. 2007; 104:7927–7932. [PubMed: 17463080]
130. Van Eps N, Preininger AM, Alexander N, Kaya AI, Meiler S, Meiler J, Hamm HE, Hubbell WL. *Proc Natl Acad Sci U S A*. 2011; 108:9420–9424. [PubMed: 21606326]
131. Ceruso MA, Periole X, Weinstein H. *J Mol Biol*. 2004; 338:469–481. [PubMed: 15081806]
132. Alexander NS, Preininger AM, Kaya AI, Stein RA, Hamm HE, Meiler J. *Nat Struct Mol Biol*. 2014; 21:56–63. [PubMed: 24292645]
133. Dror RO, Mildorf TJ, Hilger D, Manglik A, Borhani DW, Arlow DH, Philippsen A, Villanueva N, Yang Z, Lerch MT, Hubbell WL, Kobilka BK, Sunahara RK, Shaw DE. *Science*. 2015; 348:1361–1365. [PubMed: 26089515]
134. Flock T, Ravarani CN, Sun D, Venkatakrishnan AJ, Kayikci M, Tate CG, Veprintsev DB, Babu MM. *Nature*. 2015; 524:173–179. [PubMed: 26147082]
135. Manglik A, Kobilka B. *Curr Opin Cell Biol*. 2014; 27:136–143. [PubMed: 24534489]
136. Thaker TM, Kaya AI, Preininger AM, Hamm HE, Iverson TM. *Methods in molecular biology*. 2012; 796:133–174. [PubMed: 22052489]
137. Hamm HE, Deretic D, Arendt A, Hargrave PA, Koenig B, Hofmann KP. *Science*. 1988; 241:832–835. [PubMed: 3136547]
138. Scheerer P, Park JH, Hildebrand PW, Kim YJ, Krauss N, Choe HW, Hofmann KP, Ernst OP. *Nature*. 2008; 455:497–502. [PubMed: 18818650]
139. Van Eps N, Thomas CJ, Hubbell WL, Sprang SR. *Proceedings of the National Academy of Sciences of the United States of America*. 2015; 112:1404–1409. [PubMed: 25605908]
140. Stewart A, Fisher RA. *Progress in molecular biology and translational science*. 2015; 133:1–11. [PubMed: 26123299]

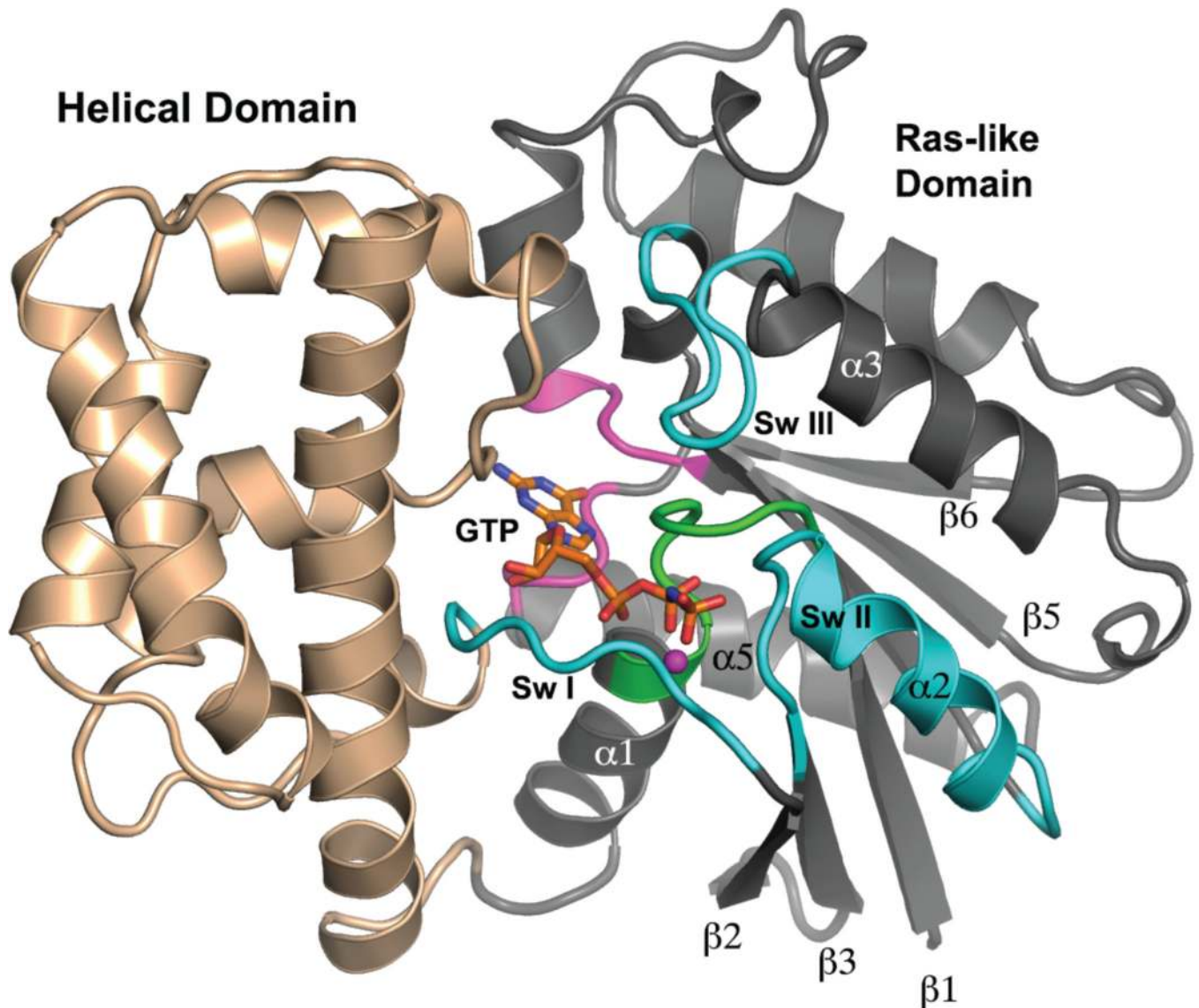


Figure 1. Tertiary structure of Gα. A model of a Gα subunit bound to GTP and Mg²⁺ is depicted as a ribbon drawing and is based on the crystal structure of Gαi1•GppNHp (PDB 1CIP). The N-terminal 31, and C-terminal 7 amino acid residues are disordered in this structure, and adopt a variety of conformations in several crystal structures, depending on crystal contacts and binding partners. The Helical domain is colored light brown and the Ras-like domain is rendered in gray. Switch segments involved in effector recognition and GTPase activity are labeled and colored cyan. The P-loop is colored green, and loop regions involved in recognition and binding of the guanine moiety of GDP and GDP are colored pink. GppNHp is shown as a stick figure, and the Mg²⁺ is represented by magenta sphere. Selected secondary structure elements in the Ras domain are labeled.

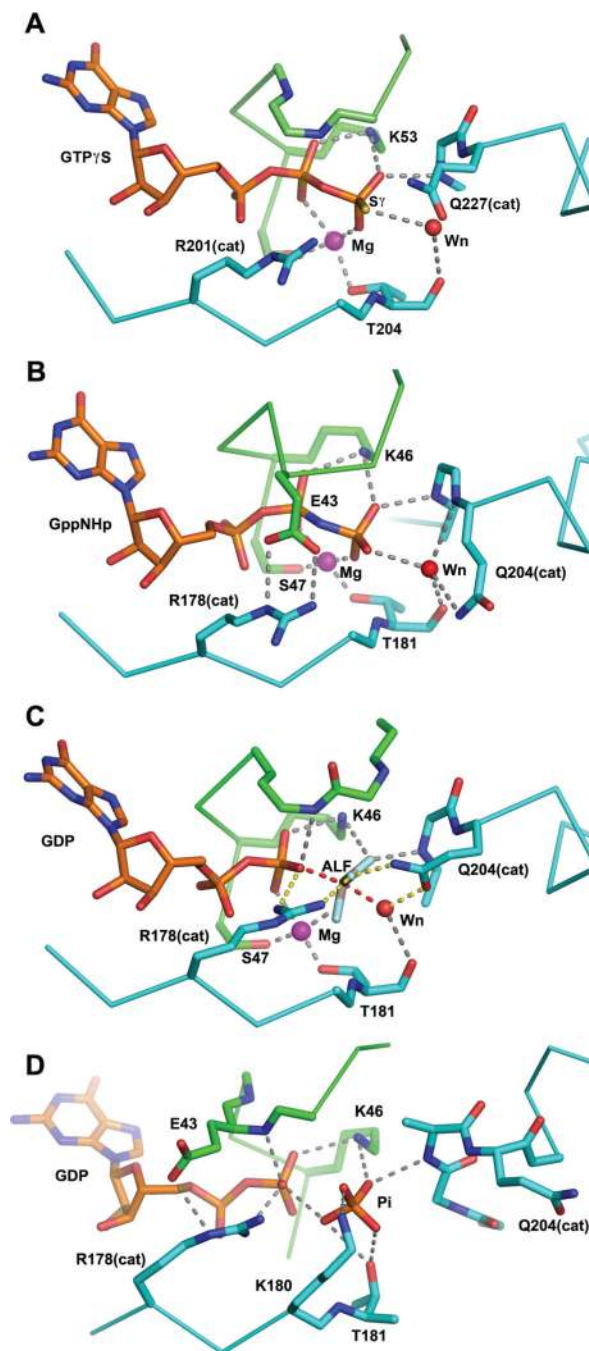


Figure 2. Snapshots of the G α catalytic site along the trajectory of GTP hydrolysis, derived from crystal structures. The coloring scheme is the same as that used in Figure 1. Nitrogen, oxygen and phosphorus atoms are colored blue, red and yellow respectively. Sulfur atoms are colored yellow. The magenta and red spheres represent magnesium ion and the water nucleophile, respectively. Residues of interest are labeled. The catalytic Gln and Arg residues are indicated with appropriate residue numbers and “cat” in parentheses. Hydrogen bonds (2.7–3.1Å) and metal-ligand coordination bonds (1.9–2.2Å) are shown as gray dashed

lines. **A**, the structure of $G\alpha_s$ bound to $GTP\gamma S$ and Mg^{2+} (PDB 1AZT, 2.3Å resolution). Note that neither of the catalytic residues Gln 227 nor Arg 201 form direct contacts with the nucleotide; **B**, the complex of $G\alpha_i1$ with $GppNHp$ and Mg^{2+} (PDB 1CIP, 1.5Å resolution). Here Arg 178 (Arg_{cat}) is restrained in a hydrogen—bonded ionic interaction with the P-loop Glu 43. Gln 204 (Gln_{cat}) is a hydrogen bond donor to the water nucleophile, thereby orienting its lone pair electrons away from the γ phosphorus. This apparently stable ground-state conformation is expected to be anti-catalytic; **C**, $G\alpha_i1$ bound to GDP, Mg^{2+} and AlF_4^- (labeled ALF), a model of the pre-organized or pre-transition state (PDB 1GFI, 2.2Å resolution; the AlF_4 moiety was not rigidly restrained to planarity during refinement). Arg_{cat} is within hydrogen bonding distance of the leaving group β - γ bridge oxygen and Gln_{cat} is a hydrogen bond donor to a fluorine (or O^-) Al substituent and accepts a hydrogen bond from the presumptive water nucleophile. The hydrogen bond network (yellow dashed lines) involving Arg_{cat} , Gln_{cat} , W_{nuc} and the the γ phosphate (modeled by ALF) orient W_{nuc} for nucleophilic attack and stabilize developing charge at the β - γ bridge leaving group oxygen (note also hydrogen bond to the latter from a P-loop amide, present also in GTP analog-bound structures); **D**, a model of the GDP, Pi ternary complex of $G\alpha$ from the crystal structure of the G203A mutant of $G\alpha_i1$ (PDB 1GIT, 2.6Å resolution). Note that switch II has reoriented and is refolded into an α helix at its N-terminus, forming an electropositive binding site for Pi. Both the β phosphate of GDP and Pi are retained in the catalytic site with multiple hydrogen bonds. The Mg^{2+} binding site is dismantled due to conformational changes in switches I and II.

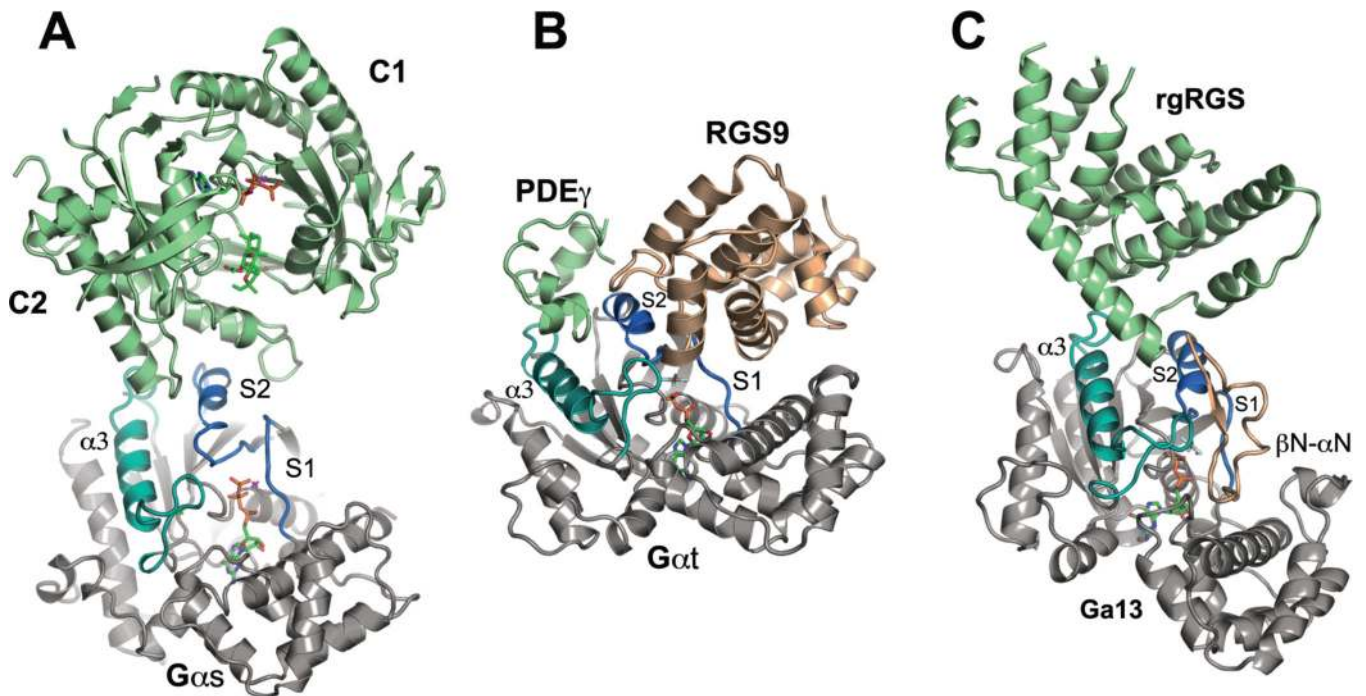


Figure 3.

Structures of G α bound to effectors and effector-GAPs. In all panels, G α is rendered in gray except switch I and II, which are colored slate blue, and the α 3 helix and switch II, which are rendered in turquoise. Effector domains are colored sage green and GAP domains are rendered in light brown. Ligands and nucleotides are rendered as stick models. **A**, structure of the catalytic domains (C1 and C2) of adenylyl cyclase bound to the GTP γ S complex of G α s (PDB 1AZS). Two helical segments of adenylyl cyclase and connecting loops engage the middle of switch II and trough between switch II and α 3; **B**, the complex between cyclic GMP phosphodiesterase γ subunit (PDE γ), the RGS domain of RGS9 and G α t/i1 (PDB 1FQK). PDE γ binds at the switch II - α 3 interface, while RGS9 occupies a distinct interface between the N-terminal half of switch II and switch I. PDE γ potentiates the GAP activity of RGS9 by stabilizing its interaction with G α ; **C**, complex of the rgRGS domain of p115RhoGEF with G α 13/i1 (PDB 1SHZ). The RGS-like domain of p115RhoGEF occupies the effector binding region of G α at the switch II - α 3 interface. The β N- α N hairpin domain that conveys GAP activity docks at the interface between the N-terminal half of switch II and switch I.

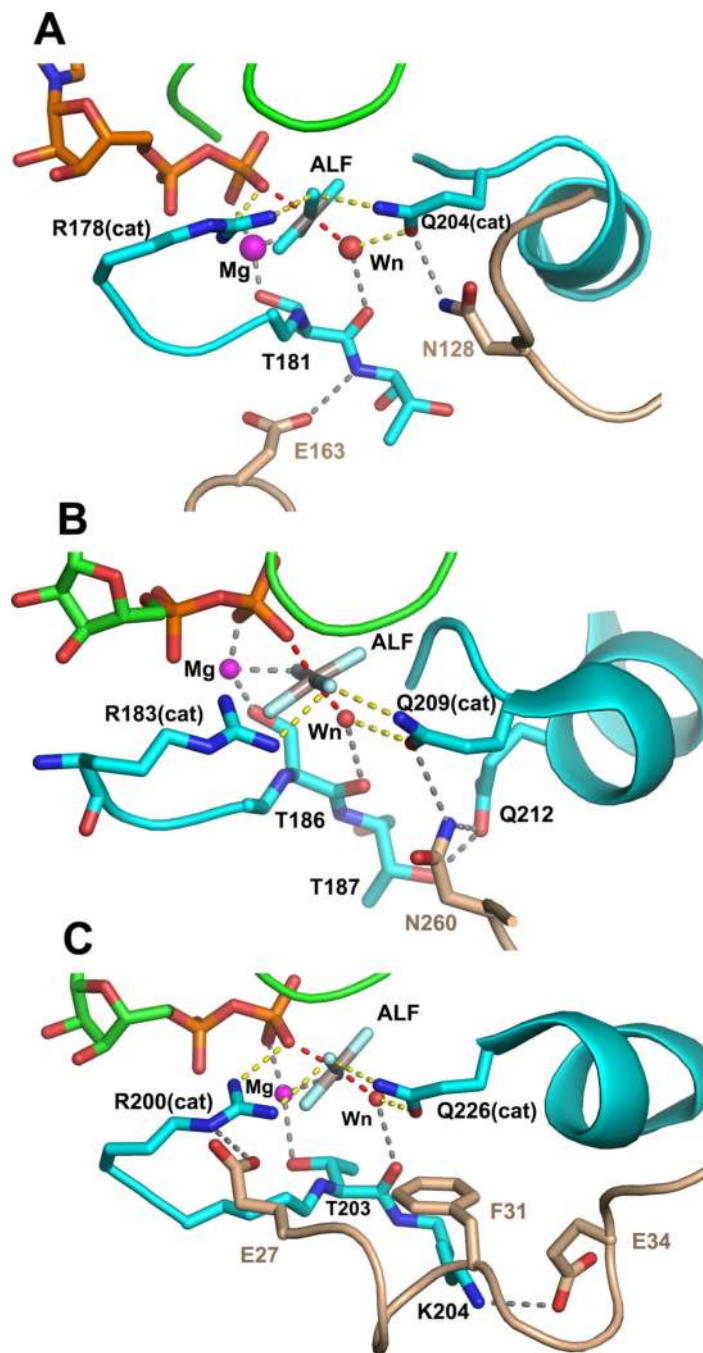


Figure 4. Interactions between $G\alpha \cdot GDP \cdot MgAlF$ active site and critical residues of RGS and effector-GAP domains. The coloring scheme used in Figures 1–3 is used. **A**, contacts between switch I and switch II of $G\alpha i1$ and RGS4 (PDB 1AGR, 2.8Å resolution) are shown. RGS residues Asn 128 and Glu 163, respectively, constrain the conformation of $G\alpha i1$ Q204 (Gln_{cat}) to the pre-transition state conformation and stabilize switch I through a hydrogen bond to the backbone amide of Thr 181; **B**, Asn 260 from the loop between the EF 3 and EF 4 domains of PLC- $\beta 3$ form a network of hydrogen bonds with residues of switch II at the catalytic site

of G α q (PDB 3OHM, 2.7Å resolution). Interactions between Asn 260 and G α q mimic that of Asn 128 of RGS4 with G α i1. The latter are strengthened by hydrogen bond network with residue Gln 212 and Thr 187 of switch I in G α q. Not shown is the extensive interaction surface of PLC- β 3 and the effector-binding surface of G α q; C, The α N segment of the β N- α N hairpin of p115RhoGEF forms hydrogen bonds with switch I and switch II in G α 13/i1. Acidic residues Glu 27 and Glu 34 form ion pair contacts with Arg_{cat} (Arg 200) and Lys 204, respectively, in switch I, stabilizing the interaction between Arg_{cat} and the fluoroaluminate, and potentially, the β - γ bridge oxygen of GTP. Phe 31 sterically restrains the position of Gln_{cat} as do Asn 128 and Asn 260 in RGS4 and PLC- β 3.

Table 1

Catalytic Residue numbers in G proteins

Protein	P-loop	switch I *	switch II *
Gαs	47 GAGESGKS	201 <u>R</u> VLT	225 GG <u>Q</u>
Gαi1	40 GAGESGKS	178 <u>R</u> VKT	202 GG <u>Q</u>
Gαt	36 GAGESGKS	174 <u>R</u> VKT	198 GG <u>Q</u>
Gαz	40 GTSNSGKS	179 <u>R</u> VKT	204 GG <u>Q</u>
Gαq	46 GTGESGKS	183 <u>R</u> VRT	207 GG <u>Q</u>
Gα13	55 GAGESGKS	200 <u>R</u> RPT	224 GG <u>Q</u>
H-Ras	10 GAGGVGKS	32 YPDT	59 AGQ

* Arg(cat) and Gln(cat) shown in italics and underlined